Advances in Radiation Oncology (2022) 7, 100980

advances in radiation oncology

www.advancesradonc.org

Research Letter

Investigating the Incidence of Pulmonary Abnormalities as Identified by Parametric Response Mapping in Patients With Lung Cancer Before Radiation Treatment

Daniel R. Owen, PhD,[a,*] Yilun Sun, PhD,[a,b] Jim C. Irrer, BS,[a] Matthew J. Schipper, PhD,[b] Caitlin A. Schonewolf, MD,[a] Stefanie Galbán, PhD,[c] Shruti Jolly, MD,[a] Randall K. Ten Haken, PhD,[a] C.J. Galbán, PhD,[c] and M.M. Matuszak, PhD[a]

[a]*Departments of Radiation Oncology, University of Michigan, Ann Arbor, Michigan;* [b]*Departments of Biostatistics, University of Michigan, Ann Arbor, Michigan;* [c]*Departments of Radiology, University of Michigan, Ann Arbor, Michigan*

Received June 13, 2021; accepted December 14, 2021

Abstract

Purpose: Parametric response mapping (PRM) of high-resolution, paired inspiration and expiration computed tomography (CT) scans is a promising analytical imaging technique that is currently used in diagnostic applications and offers the ability to characterize and quantify certain pulmonary pathologies on a patient-specific basis. As one of the first studies to implement such a technique in the radiation oncology clinic, the goal of this work was to assess the feasibility for PRM analysis to identify pulmonary abnormalities in patients with lung cancer before radiation therapy (RT).

Methods and Materials: High-resolution, paired inspiration and expiration CT scans were acquired from 23 patients with lung cancer as part of routine treatment planning CT acquisition. When applied to the paired CT scans, PRM analysis classifies lung parenchyma, on a voxel-wise basis, as normal, small airways disease (SAD), emphysema, or parenchymal disease (PD). PRM classifications were quantified as a percent of total lung volume and were evaluated globally and regionally within the lung.

Results: PRM analysis of pre-RT CT scans was successfully implemented using a workflow that produced patient-specific maps and quantified specific phenotypes of pulmonary abnormalities. Through this study, a large prevalence of SAD and PD was demonstrated in this lung cancer patient population, with global averages of 10% and 17%, respectively. Moreover, PRM-classified normal and SAD in the region with primary tumor involvement were found to be significantly different from global lung values. When present, elevated levels of PD and SAD abnormalities tended to be pervasive in multiple regions of the lung, indicating a large burden of underlying disease.

Sources of support: This work was supported in part by NIH grants P01-CA059827 (Dr Ten Haken/Lawrence), R01HL139690 (Dr C. Galban), R44HL140894 (Dr C. Galban as multi-PI), R01HL150023 (Dr C. Galban as multi-PI), and P30CA046592 (Dr C. Galban as multi-PI).

Disclosures: Dr Jolly reports consultant fees from Varian Medical Systems and AstraZeneca outside the submitted work. Dr Ten Haken reports grants from NIH during the conduct of the study, grants from Varian Medical Systems outside the submitted work. Dr C. J. Galban is a coinventor of PRM, which is licensed to Imbio by the University of Michigan. Dr Matuszak reports grants from NIH during the conduct of the study, grants and other from Varian Medical Systems outside the submitted work.

Data sharing statement: Research data are stored in an institutional repository and will be shared upon reasonable request to the corresponding author.

*Corresponding author: Daniel 'Rocky' Owen, PhD; E-mails: rockyo@umich.edu, daniel.owen@mevion.com

https://doi.org/10.1016/j.adro.2022.100980

2452-1094/© 2022 The Authors. Published by Elsevier Inc. on behalf of American Society for Radiation Oncology. This is an open access article under the CC BY-NC-ND license (http://creativecommons.org/licenses/by-nc-nd/4.0/).

Conclusions: Pulmonary abnormalities, as detected by PRM, were characterized in patients with lung cancer scheduled for RT. Although further study is needed, PRM is a highly accessible CT-based imaging technique that has the potential to identify local lung abnormalities associated with chronic obstructive pulmonary disease and interstitial lung disease. Further investigation in the radiation oncology setting may provide strategies for tailoring RT planning and risk assessment based on pre-existing PRM-based pathology.
© 2022 The Authors. Published by Elsevier Inc. on behalf of American Society for Radiation Oncology. This is an open access article under the CC BY-NC-ND license (http://creativecommons.org/licenses/by-nc-nd/4.0/).

Introduction

Patients with lung cancer are known to suffer from various pulmonary comorbidities, such as chronic obstructive pulmonary disease (COPD) or interstitial lung disease (ILD), which can diminish their ability to recover from radiation treatment and can potentially lead to severe exacerbation of the disease.[1,2] In fact, one study found that 40% to 70% of patients with lung cancer showed evidence of COPD.[3] And although ILD is generally less common (10%-20%), the outlook for patients with pre-existing ILD is dismal both in terms of survival[4] and incidence of severe toxicity.[5,6] It has also been reported that pulmonary comorbidities in patients with lung cancer are often clustered due to the shared risk factor of smoking, and patients with combined emphysema and fibrosis have the worst prognosis.[7] Despite this, the presence and severity of pulmonary comorbidities is often unknown in the radiation oncology clinic because standard practice radiation therapy (RT) planning for patients with lung cancer currently does not include any patient-specific, spatial assessment of underlying disease.

Parametric response mapping (PRM) is an analytical technique based on deformable mapping of inspiration and expiration computed tomography (CT) scans that is capable of differentiating and displaying pulmonary abnormality subtypes as a spatially resolved, patient-specific map. First introduced in 2012, PRM has been shown to improve phenotyping of COPD,[8] and studies comparing quantitative PRM metrics for both small airways disease (SAD), which is indicative of airway thickening or bronchiectasis, and emphysema, which is indicative of alveolar damage, have shown good repeatability and agreement against clinical indications obtained from the COPDgene and SPIROMICS databases.[9] Moreover, PRM-based metrics for parenchymal disease (PD), which is indicative of interstial inflammation or infection, and SAD have shown a significant association with pulmonary function tests in lung transplant recipients diagnosed with restrictive and obstructive chronic lung allograft dysfunction.[10] PRM-based estimates for SAD have also been demonstrated to be significant predictors of disease progression[11] and have been validated as a quantitative measure of SAD in patients with COPD.[12] In addition to COPD, the PRM analysis of clinical CT scans has been shown to detect PD as a measure of infection or pneumonitis in bone marrow transplant recipients and fibrosis in lung transplant recipients even in the presence of obstructive lung disease.[10,13] However, PRM assessment has yet to be implemented in patients with lung cancer before undergoing RT.

As such, the purpose of this study was to investigate the incidence of pulmonary abnormalities, as identified by PRM analysis, by quantifying voxel-wise PRM classifications for normal and abnormal lung on a global and regional basis in patients with lung cancer presenting for RT.

Methods and Materials

All patients were accrued as part of an institutional review board approved clinical trial (trial registration: clinicaltrials.gov, NCT03121287. Registered September 23, 2015. https://clinicaltrials.gov/ct2/show/NCT03121287), and informed written consent was obtained from each patient.

Twenty-three patients with lung cancer undergoing RT were accrued as part of a single-site trial. Inclusion criteria were age 18 years and older and a prescription of once daily fractionated intrathoracic RT. Exclusion criteria included RT prescriptions that were twice daily, pregnancy or lactation, and a number of criteria relevant to the magnetic resonance imaging portion of the study that are not relevant to the current study. Patients with histologically verified lung cancer scheduled for RT were eligible for enrollment. Patient characteristics are provided in Table 1.

Inspiration and expiration CT scans were performed at total lung capacity and functional residual capacity, respectively, and were acquired before any treatment. Scans were acquired at the time of RT simulation and without contrast on a Philips Big Bore 16 slice scanner. Slice thickness was 2 mm using a standardized protocol. Lung volumes, excluding the gross tumor volume, were segmented from the thoracic cavity using an in-house software. Segmented lungs were regionally divided into sextants as defined: upper lung sextants were defined as above the carina, lower lung sextants were defined as below the inferior pulmonary vein, and middle lung

Table 1 Patient characteristics and global pretreatment PRM metrics

	Total cohort (N = 23)
Histology	
Adenocarcinoma	12
Squamous cell carcinoma	8
Small cell lung cancer	2
Non-small cell lung cancer	1
Age (y)	
Median	59
Range	42-86
Sex	
Male	17
Female	6
Tumor stage	
Stage 2	1
Stage 3	18
Stage 4	4
Concurrent chemotherapy	
Yes	19
No	4
Volume (cm^3)	
Median	3513
Range	1880-5296
Mean lung dose (Gy)	
Median	13.8
Range	7.5-19.9
PRM normal (%)	
Median	64.1
Range	29.2-84.9
PRM PD (%)	
Median	12.8
Range	4.4-53.6
PRM SAD [%]	
Median	7.2
Range	0.2-28.6
PRM emphysema [%]	
Median	0.01
Range	0-2.0

Abbreviations: PD = parenchymal disease; PRM = parametric response mapping; SAD = small airways disease.

sextants were defined as between the upper and lower sextants.

PRM was applied to the paired CT scans as previously described.[8] As illustrated in Figure 1A, PRM was performed by spatially aligning the inspiration CT scan to the expiration CT scan using Elastix, an open-source, intensity-based deformable image registration algorithm.[14] Once the paired CT scans were aligned, individual voxels were classified as either normal or dysfunctional, which includes SAD, emphysema, or PD, based on the paired CT Hounsfield units (HU) and defined within the range of -1000 to -250 HU, as shown in Figure 1B.[13] In brief, voxels with values greater than or equal to -950 HU and less than -810 HU at inspiration and greater than or equal to -856 HU at expiration were classified as normal (green voxels), greater than or equal to -950 HU and less than -810 HU at inspiration and less than -856 at expiration were SAD (yellow voxels), and greater than or equal to -810 HU at inspiration were PD (purple voxels). The discrete thresholds applied to the spatially aligned paired CT scans have been previously reported and, in some cases, validated.[12,15]

PRM analysis was performed using in-house algorithms developed in a technical computing language (MATLAB v.R2016a; MathWorks Inc, Natick, MA). The percent of volume of each PRM classification was calculated by normalizing the sum of all like-classified voxels by the sum of all voxels in the lung structure (sextant or total lung) and multiplying by 100. Due to minimal levels of emphysema present in this patient population (cohort average <0.5%), only PD and SAD were reported as PRM abnormalities for this study. Based on previously published work, SAD > 20% and PD > 20% were considered significantly elevated and indicated the presence of significant pulmonary abnormality.[10,13] Correlations between PRM metrics and patient characteristics were examined using a paired *t* test. A Fisher's exact test was performed to determine whether elevated SAD or PD occurred in close proximity to the tumor (ie, sextant where the tumor resided). For all analyses, 2-sided *P* values of <.05 were considered statistically significant.

Results

The distribution of pretreatment whole-lung PRM metrics is shown in Figure 2, which corresponded to a cohort average of 62% ± 13% normal lung, 17% ± 13% PD, and 10% ± 9% SAD. A significant correlation was found between age and SAD (r = 0.46; *P* = .03); however, all other PRM metrics demonstrated negligible associations with gender, smoking status, concurrent chemotherapy, and pretreatment forced expiration volume in one second or forced vital capacity. Elevated levels of PD were found to be inversely correlated to normal parenchyma (r = -0.69; *P* < .001), which was not observed for SAD (r = -0.21; *P* = .33).

Analysis of PRM metrics over each regional sextant resulted in similar distributions to those observed over the whole lung as shown in Figure 2B. However, in the

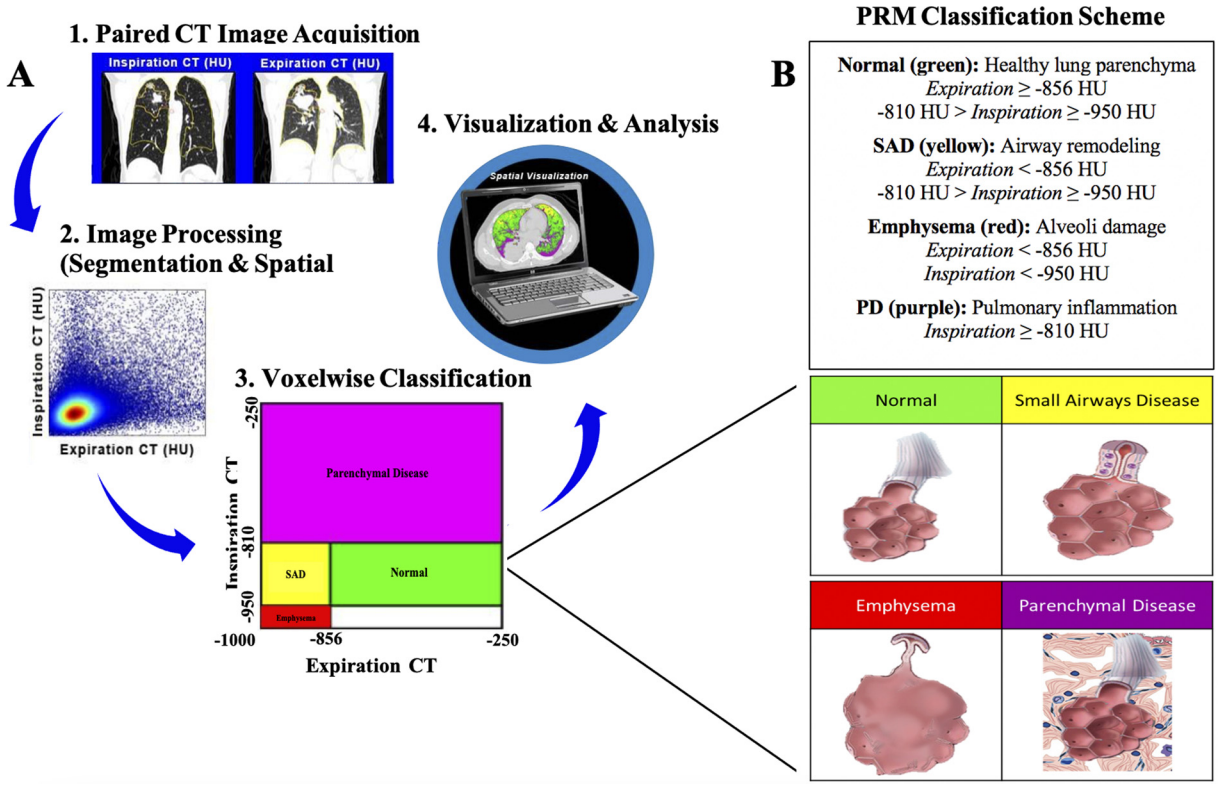

Figure 1 (A) The workflow used for PRM analysis data acquisition and processing. (B) Illustration of the pulmonary abnormalities identified by PRM analysis (bottom) and the classification schema (top) based on inspiration and expiration CT lung densities accompanied with clinical interpretations for each PRM category. *Abbreviations:* CT = computed tomography; PRM = parametric response mapping; SAD = small airways disease.

region with primary tumor involvement, average PRM values were found to be 57% ± 14% normal, 19% ± 15% PD, and 13% ± 12% SAD, and the normal (P = .04) and SAD (P = .04) values in the tumor region were found to be significantly different from global lung values. Although this patient population had a high incidence of elevated levels of PD, these abnormalities were not found to be correlated to any specific lung sextant or tumor location (Table 2).

Applying the elevated abnormality criteria of >20% over the entire lung volume, 13 patients exhibited elevated pulmonary SAD (n = 5) or PD (n = 8), and all of these patients exhibited elevated abnormalities within multiple sextants of the lungs. Only 5 patients in this cohort did not exhibit elevated disease in any of the lung regions. Moreover, 57% of the patients exhibited either elevated SAD or PD in the region with primary tumor involvement, but only 1 patient exhibited both elevated SAD (36%) and PD (21%) in the tumor region. Three patients in this cohort ultimately developed grade 2 radiation pneumonitis and each demonstrated an accumulation of disease near the tumor (Fig 3), suggesting a possible involvement in the toxicity incidence.

Discussion

As an established diagnostic imaging technique used to identify and quantify lung-related disease, PRM analysis of inspiration/expiration CT scans has the potential to improve detection and quantification of pulmonary abnormalities. In this study, PRM analysis was used to generate global and regional estimates of pulmonary abnormalities in 23 patients with lung cancer before RT. From this cohort, 20 patients exhibited some form of elevated pulmonary abnormality present in multiple regions of the lung. As such, these findings suggest a large burden of pulmonary disease, associated with COPD and ILD, exists in patients with advanced lung cancer presenting for RT. Furthermore, these comorbidities do not appear to be associated with tumor location, but instead tend to vary on a patient-specific basis (Fig 2).

PRM analysis of CT scans was used as an indicator for a subset of pulmonary comorbidities. The strength of PRM is its ability to classify individual voxels as normal, SAD, emphysema, and PD using high-resolution inspiratory and expiratory CT scans (Fig 1). In contrast to emphysema and SAD, PRM-derived PD,

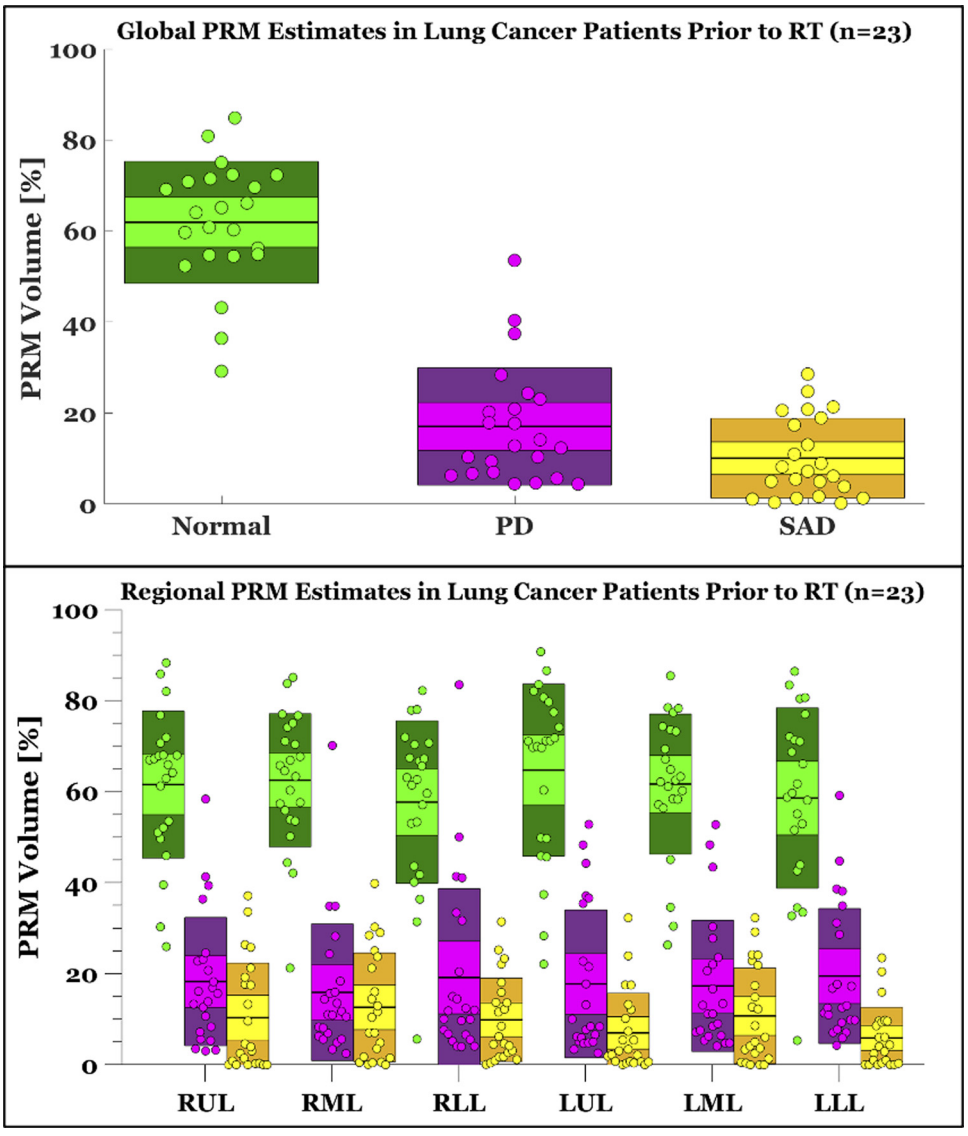

Figure 2 Global (top) and regional (bottom) parametric response mapping (PRM) classification metrics for normal, small airways disease (SAD), and parenchymal disease (PD) in 23 patients with non-small cell lung cancer before receiving radiation therapy (RT). *Abbreviations:* LLL = left lower lung; LML = left middle lung; LUL = left upper lung; RLL = right lower lung; RML = right middle lung; RUL = right upper lung.

which is classified based on -810 HU at full inflation, is less specific. This quantitative index signifies a high attenuation area initially used to account for the presence of infection in hematopoietic stem cell transplantation recipients who develop bronchiolitis obliterans syndrome.[13] Subsequently, the PD classification has been applied to quantify fibrosis and pulmonary pneumonitis.[10,16] This interpretation of PD is similar to other previously published work using similar strategies to evaluate pulmonary inflammation using high attenuation area on CT scans.[17]

The increased lung attenuation, that is, PRM-derived PD, observed in this cohort can be considered to be an indirect readout of local inflammation within the lung parenchyma. This metric has previously been applied in hematopoietic cell transplant patients and is consistent with recent studies that have correlated pre-existing local inflammation, identified on fluorodeoxyglucose-positron emission tomography, with radiation pneumonitis incidence in patients with advanced lung cancer after RT.[18,19] Other studies have also found CT-based lung density as a determinant of increased radiation-induced lung damage and have proposed personalizing RT to avoid these high density regions to improve patient outcome.[20,21] Furthermore, numerous studies have previously reported the presence of pulmonary comorbidities as a significant risk factor in the development of raidation-induced lung toxicity after RT.[22,23]

Table 2 Frequency of tumor involvement with elevated SAD and PD

Lung sextant	Primary tumor involvement	Elevated SAD	Elevated PD
RUL	8	4 (5)	1 (8)
RML	4	1 (7)	1 (5)
RLL	0	0 (4)	0 (7)
LUL	7	1 (2)	5 (8)
LML	1	0 (6)	1 (8)
LLL	3	0 (2)	0 (7)

Abbreviations: LLL = left lower lung; LML = left middle lung; LUL = left upper lung; PD = parenchymal disease; RLL = right lower lung; RML = right middle lung; RUL = right upper lung; SAD = small airways disease.
Frequency values for SAD and PD represent the number of cases with SAD > 20% and PD > 20% within the tumor-bearing lung region. Values in parentheses represent all cases with elevated SAD or PD in the given sextant.

Thus, although most functional imaging modalities have relied on quantifying perfusion and/or ventilation as a surrogate for lung function, it is possible that using PRM-based classifications may provide an enhanced understanding regarding the patient-specific risk for developing raidation-induced lung toxicity. To better understand and act upon these specific abnormalities in individual patients, 3-dimensional voxel-wise maps displaying the PRM classifications can be generated and presented to the radiation oncology team as a tool for both qualitative and quantitative assessment of pulmonary condition (Fig 4).

As an exploratory assessment for the use of PRM analysis in therapeutic applications, the primary limitation of this study was the limited number of patients included, which restricted the ability to determine the expected distribution of PRM-identified pulmonary abnormalities and any potential association with negative outcomes after RT. Second, patients with advanced lung cancer may have difficulty performing the required breath holds, sometimes up to 30 seconds, during CT acquisition. However, the CT protocols used in this

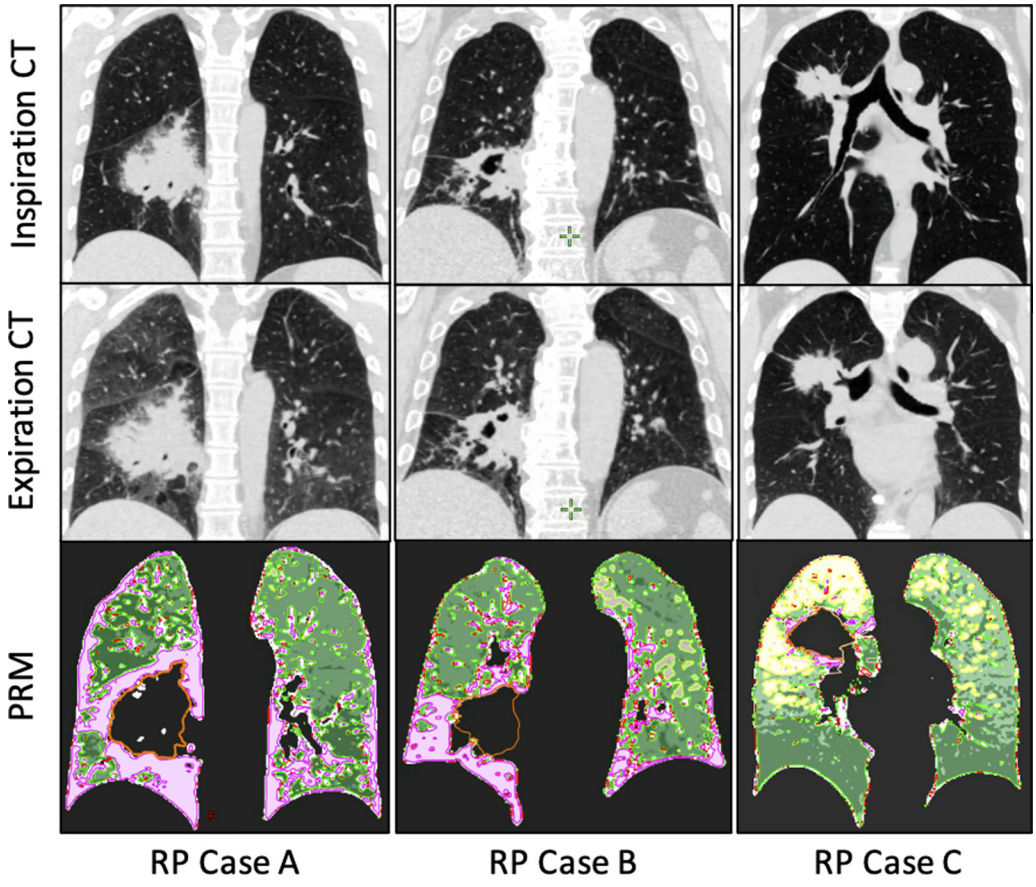

Figure 3 Single slice images for the inspiration (top row) and expiration (middle row) CT scans and parametric response mapping PRM classification distributions (bottom row) of normal parenchyma (green), small airways disease (yellow), and parenchymal disease (purple) in the 3 patients with lung cancer who incurred grade 2 radiation pneumonitis. *Abbreviations:* CT = computed tomography; PRM = parametric response mapping; RP = radiation pneumonitis.

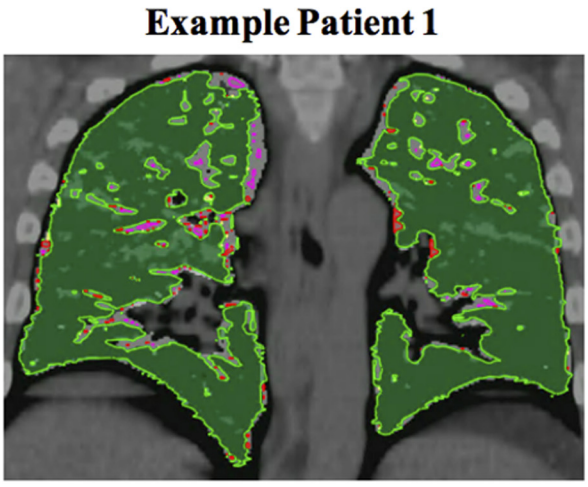

Example Patient 1 – PRM Data

Lung Structure	Normal [%]	SAD [%]	PD [%]
Global Lung	84.9	5.0	4.7
RUL	88.3	3.0	5.3
RML	83.7	4.8	4.9
RLL	82.2	8.5	4.0
LUL	90.7	0.4	4.8
LML	78.3	8.6	4.1
LLL	80.4	9.8	4.3

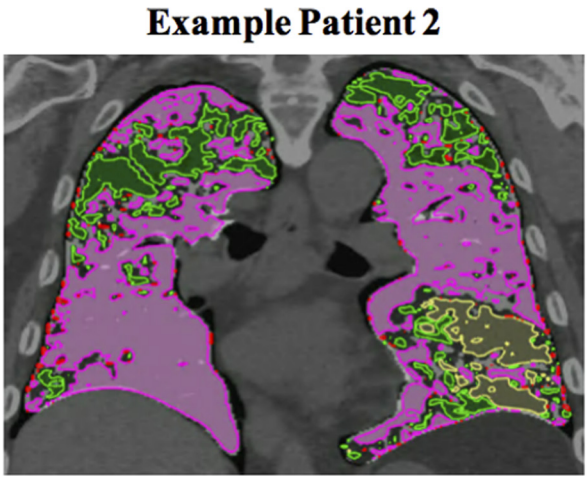

Example Patient 2 – PRM Data

Lung Structure	Normal [%]	SAD [%]	PD [%]
Global Lung	29.2	5.5	53.6
RUL	49.7	0.0	41.3
RML	21.3	0.5	70.1
RLL	5.6	0.4	83.5
LUL	45.9	1.9	35.4
LML	26.3	14.9	48.3
LLL	32.7	9.6	38.6

Figure 4 LDA visualization provided through collaboration with Imbio, LLC. Quantitative estimates are shown for the global and regional lung structures (top), and the spatial distribution is displayed across various slice orientations (bottom). *Abbreviations:* LDA = lung density analysis; LLL = left lower lung; LML = left middle lung; LUL = left upper lung; PD = parenchymal disease; PRM = parametric response mapping; RLL = right lower lung; RML = right middle lung; RUL = right upper lung; SAD = small airways disease.

study are standard for evaluating patients with chronic lung disease in thoracic radiology, and the feasibility of acquiring paired CT has been demonstrated in many large clinical trials. Finally, although PRM metrics were generally found to increase in the region of primary tumor involvement, the effect of the tumor microbiology on PRM results are unknown, and it is likely that the peritumoral area may involve inflammation of a different etiology than in the rest of the lung.

Conclusions

PRM analysis of high-resolution, paire inspiration and expiration CT scans was used to quantify pulmonary abnormalities in patients with lung cancer before undergoing RT. Although larger scale studies are needed to decipher the true potential for these PRM metrics in the management and risk assessment of patients with lung cancer undergoing RT, this study provides a blueprint for an exciting new approach to quantify pulmonary abnormalities in patients with lung cancer before, during, and after treatment, which may prove useful in the radiation oncology clinic as the basis for spatial prioritization in personalized RT planning and risk assessment. Future studies in these areas are ongoing.

Acknowledgments

The authors gratefully acknowledge the support of Chris Maurino for his role in organizing and maintaining patient information and outcome data.

Supplementary materials

Supplementary material associated with this article can be found in the online version at doi:10.1016/j.adro.2022.100980.

References

1. Asmis TR, Ding K, Seymour L, et al. Age and comorbidity as independent prognostic factors in the treatment of non-small-cell lung cancer: A review of National Cancer Institute of Canada Clinical Trials group trials. *J Clin Oncol*. 2008;26:54–59.
2. Gould MK, Munoz-Plaza CE, Hahn EE, Lee JS, Parry C, Shen E. Comorbidity profiles and their effect on treatment selection and survival among patients with lung cancer. *Annal Am Thorac Soc*. 2017;14:1571–1580.
3. Leduc C, Antoni D, Charloux A, Falcoz PE, Quoix E. Comorbidities in the management of patients with lung cancer. *Eur Resp J*. 2017:49.
4. Han SY, Lee YJ, Park JS, et al. Prognosis of non-small-cell lung cancer in patients with idiopathic pulmonary fibrosis. *Sci Rep*. 2019;9:1–10.
5. Ozawa Y, Abe T, Omae M, et al. Impact of preexisting interstitial lung disease on acute, extensive radiation pneumonitis: Retrospective analysis of patients with lung cancer. *PloS One*. 2015;10:e0140437.
6. Bahig H, Filion E, Vu T, et al. Severe radiation pneumonitis after lung stereotactic ablative radiation therapy in patients with interstitial lung disease. *Pract Radiat Oncol*. 2016;6:367–374.
7. Usui K, Tanai C, Tanaka Y, Noda H, Ishihara T. The prevalence of pulmonary fibrosis combined with emphysema in patients with lung cancer. *Respirology*. 2011;16:326–331.
8. Galbán CJ, Han MK, Boes JL, et al. Computed tomography–based biomarker provides unique signature for diagnosis of COPD phenotypes and disease progression. *Nat Med*. 2012;18:1711–1715.
9. Martinez CH, Diaz AA, Meldrum C, et al. Age and small airway imaging abnormalities in subjects with and without airflow obstruction in spiromics. *Am J Respir Crit Care Med*. 2017;195:464–472.
10. Belloli EA, Degtiar I, Wang X, et al. Parametric response mapping as an imaging biomarker in lung transplant recipients. *Am J Respir Crit Care Med*. 2017;195:942–952.
11. Bhatt SP, Soler X, Wang X, et al. Association between functional small airway disease and FEV_1 decline in chronic obstructive pulmonary disease. *Am J Respir Crit Care Med*. 2016;194:178–184.
12. Vasilescu DM, Martinez FJ, Marchetti N, et al. Noninvasive imaging biomarker identifies small airway damage in severe chronic obstructive pulmonary disease. *Am J Respir Crit Care Med*. 2019;200:575–581.
13. Galban CJ, Boes JL, Bule M, et al. Parametric response mapping as a diagnostic indicator of bronchiolitis obliterans syndrome. *Biol Blood Marrow Transplant*. 2014;20:1592–1598.
14. Klein S, Staring M, Murphy K, Viergever MA, Pluim JPW. Elastix: A toolbox for intensity-based medical image registration. *IEEE Trans Med Imaging*. 2010;29:196–205.
15. Mascalchi M, Camiciottoli G, Diciotti S. Lung densitometry: Why, how and when. *J Thorac Dis*. 2017;9:3319–3345.
16. Sharifi H, Yu KL, Guo H, et al. Machine learning algorithms to differentiate among pulmonary complications after hematopoietic cell transplant. *Chest*. 2020;158:1090–1103.
17. Podolanczuk AJ, Oelsner EC, Barr RG, et al. High attenuation areas on chest computed tomography in community dwelling adults: The MESA study. *Eur Resp J*. 2016;48:1442–1452.
18. Castillo R, Pham N, Ansari S, et al. Pre-radiotherapy FDG PET predicts radiation pneumonitis in lung cancer. *Radiat Oncol*. 2014;9:74.
19. Chaudhuri AA, Binkley MS, Rigdon J, et al. Pre-treatment non-target lung FDG-PET uptake predicts symptomatic radiation pneumonitis following stereotactic ablative radiotherapy (SABR) pre-treatment non-target lung FDG-PET uptake predicts radiation pneumonitis after SABR. *Radiother Oncol*. 2016;119:454–460.
20. Defraene G, van Elmpt W, Crijns W, Slagmolen P, De Ruysscher D. CT characteristics allow identification of patient-specific susceptibility for radiation-induced lung damage. *Radiother Oncol*. 2015;117:29–35.
21. Defraene G, van Elmpt W, Crijns W, De Ruysscher D. Regional variability in radiation-induced lung damage can be predicted by baseline CT numbers. *Radiother Oncol*. 2017;122:300–306.
22. Appelt AL, Vogelius IR, Farr KP, Khalil AA, Bentzen SM, Bentzen M. Towards individualized dose constraints: Adjusting the QUANTEC radiation pneumonitis model for clinical risk factors. *Acta Oncol*. 2014;53:605–612.
23. Kimura T, Doi Y, Nakashima T, et al. Combined ventilation and perfusion imaging correlates with the dosimetric parameters of radiation pneumonitis in radiation therapy planning for lung cancer. *Int J Radiat Oncol Biol Phys*. 2015;93:778–787.